

References

- ¹ Buffalano, C., "A Physical Model of the Apollo Oxygen Releases," *Journal of Geophysical Research*, Vol. 76, 1971, p. 27.
- ² Sharma, R. and Buffalano, C., "Temperature and Size Histories of Liquid H₂, O₂, and H₂O Particles Released in Space," *Journal of Geophysical Research*, Vol. 76, 1971, p. 232.
- ³ Van DeHulst, H., *Light Scattering by Small Particles*, Wiley, New York, 1957.

Development of the Astrobee F Sounding Rocket System

R. B. JENKINS* AND J. P. TAYLOR†

Aerojet Liquid Rocket Company, Sacramento, Calif.

H. J. HONECKER JR.‡

NASA Goddard Space Flight Center, Greenbelt, Md.

Introduction

THE Astrobee F sounding rocket vehicle was developed from a dual-thrust, long-burning, solid propellant rocket motor developed for the NASA Office of Aeronautics and Space Technology to demonstrate new propulsion technology. The concept for a dual-thrust extended burning solid rocket motor grew out of earlier studies performed for NASA-OAST. The first application of these concepts was the development of the 6-in. diameter dual-thrust Astrobee D which has previously been reported.¹ The Astrobee F propulsion system was an extension of the design concept utilizing hydroxyl-terminated polybutadiene (HTPB) propellant designed to have very low burning rates. A relatively neutral pressure history is maintained during the sustain portion of burning by use of a one piece molded plastic ablating nozzle.

An abbreviated static test program included four static firings augmented by a well-instrumented flight test which featured an attempt to recover the motor as well as the payload. Thus, the first flights of the vehicle became "high altitude static tests." Upon successful demonstration of the Astrobee F propulsion

system, a vehicle design and flight test program was initiated by NASA Goddard Space Flight Center for the demonstration of the propulsion system as part of a complete sounding rocket vehicle (Fig. 1).

Motor Development

The general concept of the Astrobee F was similar to that of the Astrobee D, in that the motor provides a dual-thrust level; a short, high-thrust level boost-phase followed by a relatively long, low-thrust level sustain phase. The extended sustain phase was to provide the advantages of a low level of drag, aerodynamic heating, and dynamic pressure, all of which have a significant effect on payload design and environment. The Astrobee F environment is similar to the liquid Aerobees.

There was concern that a one piece molded plastic nozzle similar to that used on the Astrobee D might not be scalable for use on a significantly larger size Astrobee F motor. Variations in molding technique, materials preparation and post cure were tried. These tests resulted in the largest known single piece molded nozzle. The nozzle, which is of a 13.5-in.-diam, uses 49 lb of glass phenolic material. The nozzle section thickness tapers from 3.5 in. to 0.5 in.

The first Astrobee F motor was fired on Dec. 2, 1970. The motor achieved the desired propulsion parameters and burned for a duration of 50 sec. Examination of the motor after firing, showed the internal insulation had eroded at a localized area in the aft section of the motor and that the case material had been heated to the point of distortion. Examination of the liner revealed that material remained through approximately 270° of the aft portion of the chamber, but that all material had been removed in a portion of one quadrant. A number of potential causes for this asymmetrical erosion were considered and what appeared to be a reasonable hypothesis was formulated.

The second unit was fired on Feb. 18, 1971. Propulsion-wise, it appeared to be nearly identical to FF01 with a smooth transition between the high-pressure boost and the low-pressure sustain portion, as predicted. Operation was normal through approximately 42 sec when the chamber pressure took a sharp drop. Upon examination, the motor was found to have burned through in one quadrant in the aft portion of the chamber. Subsequent examination of the linear system revealed an identical erosion pattern to that of FF01. That is, adequate insulation through three quadrants with one quadrant having been reduced to zero insulation. It became apparent from the results of this

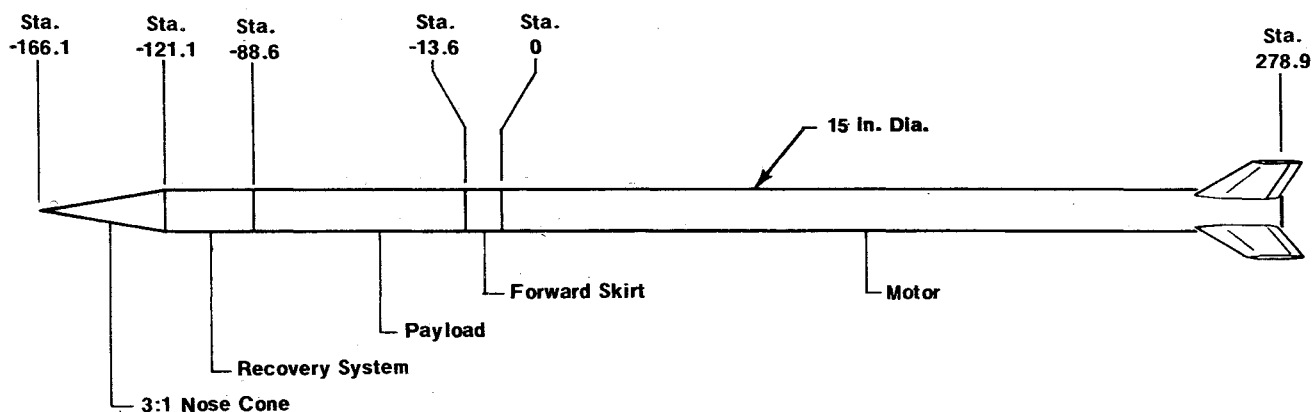


Fig. 1 Astrobee F flight test vehicle.

Presented as Paper 73-300 at the AIAA 3rd Sounding Rocket Technology Conference, Albuquerque, N.Mex., March 7-9, 1973; submitted April 13, 1973; revision received July 27, 1973.

Index categories: LV/M Propulsion System Integration; Sounding Rocket Systems; Solid and Hybrid Rocket Engines.

* Manager Astrobee Programs.

† Manager Engineering Analysis and Special Programs.

‡ Program Manager Performance Branch Sounding Rocket Division.

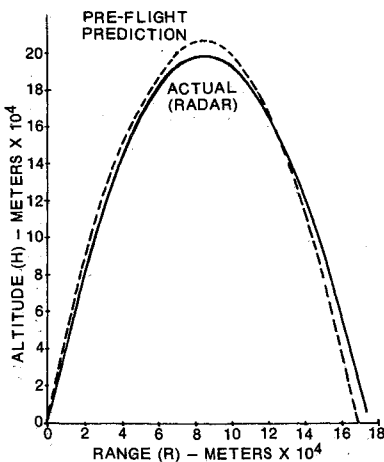


Fig. 5 Flight test vehicle trajectory.

3) Burnout roll rate was 3.4 rev/sec; the fins were set to produce a theoretical 2.5 rps. However, fin conduit facing interference effects were unaccounted for.

4) Burnout velocity was 1737 m/sec at an altitude of 48 km; predicted values were 1772 m/sec and 46 km. Performance was near predicted (Fig. 5).

5) Longitudinal acceleration averaged about 11.5g during boost phase, dropped to about 1g at boost phase burnout, then rose to a sustain phase maximum of about 6.3g at $t + 38$ sec.

6) No significant temperature rise occurred anywhere on the motor during burn. Payload temperature was of the order of magnitude expected (Fig. 6).

7) Vibration input to the payload, once the vehicle was out of the tower, varied from about 1.2g to about 4g, peak to peak, at about 1 kHz in the lateral planes and from about 1.5g to 3g, 1 kHz in the thrust direction.

8) The vehicle exited the tower at $t + 0.96$ sec with a velocity of 84.5 m/sec.

9) The two lateral accelerometers in the tail show a peak to peak vibration of 10g–12g at moderate frequencies. The apparent correlation between the amplitude-time characteristic of this vibration and the dynamic pressure vs time curve suggests that the observed vibration is influenced by, perhaps dominated by, aerodynamics rather than the motor and is most likely due to interactive flow phenomena between the conduits and the fins which were not aligned with each other.

10) The recovery of the vehicle failed because the fins were not jettisoned.

The main parachute, its bag, the flotation bag and its bag, and portions of the drogue chute bag were recovered. Entangled in the mass of nylon and webbing were a number of fragments from the recovery system itself and from the payload, indicating that the vehicle payload section of the vehicle disintegrated at impact.

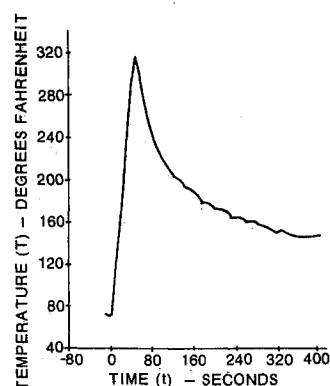


Fig. 6 Forward skirt door temperature.

Summary

A successful program for the demonstration of a new propulsion system with the stated new technology features and the integration of this motor into a flight vehicle was accomplished.

References

- ¹ Jenkins, R. B. and Taylor, J. P., "Astrobee D—An Advanced Technology Boost/Sustain Meteorological Rocket Vehicle," AIAA Paper 70-1387, Williamsburg, Va., 1970.
- ² Coanda, H., "Analysis of Thrust Due to the Coanda Phenomenon," Contract Rept. AF 61(052)-382, Oct. 29, 1960, U.S. Air Force, Washington, D.C.

Blowing Simulation of Asymmetric Transition Effects on Slender Ablating Vehicles

LARS E. ERICSSON*

Lockheed Missiles & Space Company, Inc., Sunnyvale, Calif.

THE effects of aft body asymmetric transition on slender vehicle aerodynamics as measured by Martellucci and Neff,¹ using blowing to simulate ablative mass addition, seem to be in sharp contrast to what has been presented in Ref. 2 (see Fig. 1). The negative aerodynamic loading induced by asymmetric transition should have the highest slope at $\alpha = 0$ and not at some intermediate value like $\alpha = 0.5^\circ$.

In order to understand the peculiar behavior of the transition-induced characteristics in Fig. 1, the author consulted the data source.³ As sketched in the insets in Fig. 2, there are two important α -parameters in a test simulating asymmetric transition effects on an ablating model using blowing. The blowing area was shaped to conform to the free transition front measured on the nonblowing solid model (with smooth surface) at a certain angle of attack $\alpha = \alpha_{AT}$. The aerodynamic loads for various blowing rates were then measured as a function of α for three blowing geometries, i.e., those with blowing fronts corresponding to the transition lines for $\alpha_{AT} = 0^\circ, 1^\circ$, and 2° . The freestream unit Reynolds number was kept constant at the value used when defining the transition front geometry on the solid model.

Even when the transition front is far upstream of the base, thereby minimizing the sting interference which (otherwise) can be large for models with boundary-layer mass addition,⁴ one faces several problems when attempting this type of simulation of asymmetric transition effects, as is discussed by Martellucci and Neff.¹ Using an impervious forward section for the laminar flow region may give the turbulent blowing rate increment a larger effect than it has in presence of forebody blowing (at laminar levels). At low blowing rates the breathing and tripping effects of the porous surface itself also have to be considered.⁵⁻⁸

In spite of these simulation difficulties, one can postulate that at some angle of attack close to $\alpha = \alpha_{AT}$ the free transition effect is indeed simulated. With this in mind the author went

Presented as Appendix of AIAA Paper 73-126 at the AIAA 11th Aerospace Sciences Meeting, Washington, D.C., January 10–12, 1973; submitted April 13, 1973; revision received September 13, 1973.

Index categories: Boundary Layer Stability and Transition; Jets, Wakes, and Viscid-Inviscid Flow Interactions; Entry Vehicle Dynamics and Control.

* Consulting Engineer. Associate Fellow AIAA.

† "Free" means with transition free to move with α , as is the case on the ablating flight vehicle.